

Discretization of mixed formulations of elliptic problems on polyhedral meshes

Konstantin Lipnikov*, Gianmarco Manzini*

Abstract

We review basic design principles underpinning the construction of mimetic finite difference and a few finite volume and finite element schemes for mixed formulations of elliptic problems. For a class of low-order mixed-hybrid schemes, we show connections between these principles and prove that the consistency and stability conditions must lead to a member of the mimetic family of schemes regardless of the selected discretization framework. Finally, we give two examples of using flexibility of the mimetic framework: derivation of higher-order schemes and convergent schemes for nonlinear problems with small diffusion coefficients.

1 Introduction

The mixed formulation allows us to calculate simultaneously the primary solution of a PDE and its flux. For this reason, mixed formulations are very useful for numerical solution of multiphysics systems. The focus of this work is on a single diffusive process that is a part of almost any complex multiphysics system.

In this paper, we present design principles used in the derivation of mimetic finite difference (MFD) schemes on polygonal and polyhedral meshes and establish bridges to design principles used by a few other discretization frameworks (finite volumes and finite elements). The focus on the design principle allows us to avoid technical details and provide a more clear connection between different frameworks in comparison with the work performed in [26]. We also illustrate the flexibility of the mimetic framework with two challenging examples: derivation of arbitrary-order accurate schemes for linear problems and convergent schemes for nonlinear problems with degenerate diffusion coefficients.

Many ideas underpinning the MFD method were originally formulated in the sixties for orthogonal meshes using the finite difference framework from which the name of the method was derived. Over the years, the MFD method has been extensively developed for the solution of a wide range of scientific and engineering problems in continuum mechanics [39], electromagnetics [32, 34], fluid flows [36, 7, 8, 17, 6], elasticity [5, 10], obstacle and control problems [3, 1, 2], diffusion [33], discretization of differential forms [11, 41, 12], and eigenvalue analysis [15]. An extensive list of people who contributed to the development

¹Applied Mathematics and Plasma Physics Group, Theoretical Division, Los Alamos National Laboratory, {lipnikov,manzini}@lanl.gov

of the MFD method can be found in the recent book [9] and review paper [35]. The paper summarizes almost all known results on Cartesian and curvilinear meshes for various PDEs including the Lagrangian hydrodynamics. The book complements the paper by providing numerous examples and describing basic tools used in the convergence analysis of mimetic schemes for elliptic PDEs.

The MFD method preserves or mimics essential mathematical and physical properties of underlying partial differential equations (PDEs) on general polygonal and polyhedral meshes. For the elliptic equation, these properties include the *local flux balance* and the *duality between gradient and divergence operators*. The latter implies symmetry and positive definiteness of the resulting matrix operator and is desirable for robustness and reliability of numerical simulations. The duality of the primary and derived mimetic operators is one of the major design principles. The *definition of the primary mimetic operators is coordinate invariant*, which is another design principle that allows us to build discrete schemes for non-Cartesian coordinate systems. The discrete operators are also built to satisfy *exact identities*, the property that is critical for avoiding spurious numerical solutions, providing accurate modeling of conservation laws, and making the convergence analysis possible.

The related discretization frameworks considered in this paper include the finite volume methods [29, 25], the mixed finite element (MFE) method [42], and the virtual element method (VEM) [13]. Other finite volume frameworks exist that are based on mimetic principles such as the discrete duality finite volume methods (DDFV), see, e.g., [23, 20], but these methods do not fit in the MFD framework and will not be considered here.

The FV methods, originally introduced in [27, 28] for the heat equation and dubbed as the integrated finite difference method, form, perhaps, the largest class of schemes that can handle unstructured polygonal and polyhedral meshes, non-linear problems, and problems with anisotropic coefficients. An introduction to the finite volume methodology can be found in the recent review [24]. Almost all FV methods start with a discrete representation of the flux balance equation. This representation is exact and this property is so important that all the methods that we consider in this paper use the same discrete form of the balance equation and the difference between them is only in the discretization of the constitutive equation.

The classical cell-centered FV scheme uses a two-point flux formula that is second-order accurate for special meshes such as the Voronoi tessellations. To overcome this limitation, a class of FV methods, consistent by design, is proposed by introducing additional unknowns on mesh faces. Examples of such methods are the *hybrid finite volume* method [29], and the *mixed finite volume* method [25]. These FV methods start with different definitions of the cell-based discrete gradient that are exact for linear solutions. The formula for the numerical flux based on this gradient needs a stabilization term. Construction of the stabilized flux uses two principles. First, the stabilization term should be zero on linear solutions. Second, the stabilized flux is defined as the solution of a certain equation with a symmetric and positive definite bilinear form. We will show that these design principles imply the duality principle in the mimetic framework.

The VEM was originally introduced as an evolution of the MFD method. In the classical finite element spirit, the duality principle is incorporated directly in the weak formulation. The exact identities are replaced by the exact sequence of virtual finite element spaces. A new design principle is the unisolvency property where the space of degrees of freedom

is isomorphic to a space of finite element functions and includes polynomial as well as non-polynomial functions. The bilinear forms are split explicitly into consistency and stability forms using problem-dependent L^2 and H^1 projectors. We discuss how the new design principles are connected to the stability and consistency conditions in the mimetic framework.

The recent developments of the MFD framework exploit its flexibility for selecting non-standard degrees of freedom, optimization of inner products, and non-standard approximations of primary operators to build schemes with higher order of accuracy and convergence schemes for nonlinear PDEs with degenerate coefficients (see also Section 4.2).

Extension to higher-order mixed scheme is almost straightforward in the mimetic framework. The key step is the proper selection of degrees of freedom that (a) simplify the discretization of the primary divergence operator and (b) allows us to formulate a computable consistency condition. A new design principle is introduced in this case, which states that a commuting relation exists between the interpolation operators defining the degrees of freedom of scalar and vector fields, and the divergence operators in the discrete and continuum settings.

All of the aforementioned methods discretize effectively the divergence operator “ $div(\cdot)$ ”. To solve nonlinear parabolic equations, we employ new MFD schemes where the primary operator discretizes the combined operator “ $div k(\cdot)$ ”, where k is the non-constant scalar diffusion coefficient. The resulting scheme uses both cell-centered and face-centered values of the diffusion coefficient. This model has applications in heat diffusion [18] and moisture transport in porous media [43]. The duality property mentioned above guarantees that the schemes can be formulated as algebraic problems with symmetric and positive definite matrices. Matrices with these properties lead to better performance of scalable iterative solvers, such as algebraic multigrid solvers and Krylov solvers such as the preconditioned conjugate gradient.

Finally, we mention other discretization methods that work on general meshes. Our necessarily incomplete list include the polygonal/polyhedral finite element method (PFEM) [48, 46, 45, 47, 38], hybrid high-order method [22], the discontinuous Galerkin (DG) method [21], hybridized discontinuous Galerkin (HDG) method [19], and the weak Galerkin (wG) method [49].

The outline of the paper is as follows. In Section 2, we review the basic discretization principles of the mimetic framework. In Section 3, we derive the mimetic finite difference method for elliptic problems through the consistency and stability properties. We also prove that any mixed-hybrid method that uses the same degrees of freedom leads to a member of the mimetic family of schemes. In Section 4, we review the recent progress in the development of mimetic methods for mixed formulations of elliptic problems. Our final remarks and conclusions are given in Section 5.

2 Principles of the mimetic discretization framework

The MFD method mimics important mathematical and physical properties of underlying PDEs. We give two examples showing the importance of preserving such properties in physics simulations.

Consider a polygonal or polyhedral mesh Ω_h . We denote the sets of mesh nodes, edges, faces, and cells by symbols \mathcal{N} , \mathcal{E} , \mathcal{F} and \mathcal{C} , respectively, the set of vectors collecting the degrees of freedom associated with those mesh objects by the corresponding symbol with the subscript “ h ”, and the restriction to cell “ c ” by the subscript “ h, c ”. Each set of vectors of degrees of freedom with the (obvious) definitions of addition and multiplication by a scalar number is a linear space. For example, \mathcal{F}_h is the linear space of vectors formed by the degrees of freedom located on the mesh faces, and $\mathcal{F}_{h,c}$ is its restriction to cell c . Its precise definition depends on the scheme. An illustration of particular discrete spaces restricted to a single cell is shown in Fig. 1.

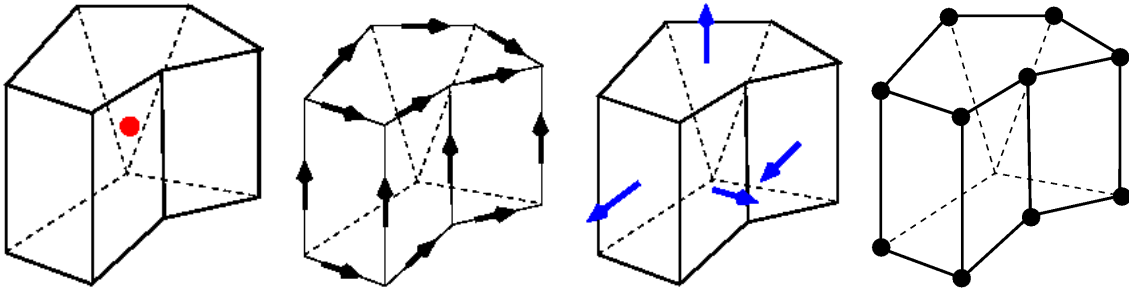


Figure 1: Illustration of the degrees of freedom in low-order mimetic schemes. The local spaces associated with cell c from left to right are $\mathcal{C}_{h,c}$, $\mathcal{E}_{h,c}$, $\mathcal{F}_{h,c}$, $\mathcal{N}_{h,c}$. The degrees of freedom are shown only on the visible objects.

The mimetic finite difference method operates with discrete analogs of the first-order operators. These operators are designed to satisfy exact identities and duality principles.

2.1 Global mimetic operators

In the mimetic framework, we usually discretize pairs of adjoint operators, such as the primary divergence $\mathcal{DIV}: \mathcal{F}_h \rightarrow \mathcal{C}_h$ and the derived gradient $\widetilde{\mathcal{GRAD}}: \mathcal{F}_h \rightarrow \mathcal{C}_h$. Hereafter, we will distinguish the derived operators from the primary operators by using a tilde on the operator’s symbol. It is convenient to think about these operators as matrices acting between finite dimensional linear spaces. To discretize a large class of PDEs, we need three pairs of primary and derived operators, which are discrete analogs of gradient, curl and divergence operators. Each pair of operators satisfies a discrete integration by parts formula, e.g.

$$[\mathcal{DIV} \mathbf{u}_h, q_h]_{\mathcal{C}_h} = -[\mathbf{u}_h, \widetilde{\mathcal{GRAD}} q_h]_{\mathcal{F}_h} \quad \forall \mathbf{u}_h \in \mathcal{F}_h, \forall q_h \in \mathcal{C}_h. \quad (2.1)$$

This formula represents one of the mimetic discretization principles as it mimics the continuum Green formula

$$\int_{\Omega} (\operatorname{div} \mathbf{u}) q \, dx = - \int_{\Omega} \mathbf{u} \cdot \nabla q \, dx \quad \forall \mathbf{u} \in H_{div}(\Omega), \forall q \in H_0^1(\Omega). \quad (2.2)$$

The brackets $[\cdot, \cdot]_{\mathcal{C}_h}$ and $[\cdot, \cdot]_{\mathcal{F}_h}$ in (2.1) stand for an approximation of the integrals in (2.2) and will be referred to as the *mimetic inner products* (or, simply *inner products*). The inner products are typically constructed from local (e.g. cell-based or node-based) inner products, which simplifies their derivation. For example, the two inner products in (2.1) can be reformulated as

$$[\mathbf{u}_h, \mathbf{v}_h]_{\mathcal{F}_h} = \sum_{c \in \Omega_h} [\mathbf{u}_c, \mathbf{v}_c]_{\mathcal{F}_{h,c}}, \quad [p_h, q_h]_{\mathcal{C}_h} = \sum_{c \in \Omega_h} [p_c, q_c]_{\mathcal{C}_{h,c}} \quad (2.3)$$

where \mathbf{v}_c , \mathbf{u}_c , q_c and p_c denote the restriction to mesh cell c of the corresponding global vectors in the left-hand side and $[\cdot, \cdot]_{\mathcal{F}_{h,c}}$ and $[\cdot, \cdot]_{\mathcal{C}_{h,c}}$ are the local contribution from c to the global inner products $[\cdot, \cdot]_{\mathcal{F}_h}$ and $[\cdot, \cdot]_{\mathcal{C}_h}$, respectively.

Let $\mathbf{M}_{\mathcal{C}}$ and $\mathbf{M}_{\mathcal{F}}$ be the symmetric positive definite matrices induced by the inner products $[\cdot, \cdot]_{\mathcal{C}_h}$ and $[\cdot, \cdot]_{\mathcal{F}_h}$, respectively. Then, the explicit formula for the derived gradient operator is

$$\widetilde{\mathcal{GRAD}} = -\mathbf{M}_{\mathcal{F}}^{-1} \mathcal{DIV}^T \mathbf{M}_{\mathcal{C}}.$$

This formula shows that this operator has a nonlocal stencil when matrix $\mathbf{M}_{\mathcal{F}}$ is irreducible as is typical for unstructured meshes. Note that the same property holds true for many other discretization frameworks.

Formula (2.1) implies that in general the discrete operators cannot be discretized independently. If we discretize one of the operators, e.g., the divergence, and select the inner products, the other operator, the gradient, must be derived from formula (2.1). The existing freedom is in the selection of the inner products.

The selection of the discrete spaces is typically done to simplify the discretization of the primary mimetic operator. For a different pair of discrete spaces, e.g., \mathcal{N}_h and \mathcal{E}_h , one can find that the gradient operator can be discretized in a natural way. In such a case, the gradient operator $\mathcal{GRAD}: \mathcal{N}_h \rightarrow \mathcal{E}_h$ is the primary mimetic operator and the discrete divergence operator $\widetilde{\mathcal{DIV}}: \mathcal{E}_h \rightarrow \mathcal{N}_h$ is the derived operator. This pair of operators satisfies another discrete integration by parts formula that mimics (2.2):

$$[\widetilde{\mathcal{DIV}} \mathbf{v}_h, p_h]_{\mathcal{N}_h} = -[\mathbf{v}_h, \mathcal{GRAD} p_h]_{\mathcal{E}_h} \quad \forall p_h \in \mathcal{N}_h, \quad \forall \mathbf{v}_h \in \mathcal{E}_h. \quad (2.4)$$

The explicit formula for the derived divergence operator is

$$\widetilde{\mathcal{DIV}} = -\mathbf{M}_{\mathcal{N}}^{-1} \mathcal{GRAD}^T \mathbf{M}_{\mathcal{E}},$$

where $\mathbf{M}_{\mathcal{E}}$ and $\mathbf{M}_{\mathcal{N}}$ are symmetric positive definite matrices induced by the inner products. Note that in some low-order mimetic schemes, matrix $\mathbf{M}_{\mathcal{N}}$ is diagonal, so that the derived operator has a local stencil.

The third pair of discrete operators approximates the continuum operators “curl”. Let $\mathcal{CURL}: \mathcal{E}_h \rightarrow \mathcal{F}_h$ and $\widetilde{\mathcal{CURL}}: \mathcal{F}_h \rightarrow \mathcal{E}_h$ satisfy the discrete integration by parts formula

$$[\mathcal{CURL} \mathbf{v}_h, \mathbf{u}_h]_{\mathcal{F}_h} = [\mathbf{v}_h, \widetilde{\mathcal{CURL}} \mathbf{u}_h]_{\mathcal{E}_h} \quad \forall \mathbf{v}_h \in \mathcal{E}_h, \quad \forall \mathbf{u}_h \in \mathcal{F}_h,$$

which mimics the continuum formula

$$\int_{\Omega} (\text{curl } \mathbf{v}) \cdot \mathbf{u} \, dx = \int_{\Omega} \mathbf{v} \cdot (\text{curl } \mathbf{u}) \, dx \quad \forall \mathbf{u} \in H_{\text{curl}}^0(\Omega), \quad \forall \mathbf{v} \in H_{\text{curl}}(\Omega).$$

The explicit formula for the derived curl operator is

$$\widetilde{CURL} = M_{\mathcal{E}}^{-1} CURL^T M_{\mathcal{F}},$$

so that this derived operator has typically a non-local stencil.

The spaces of discrete functions that we have introduced so far satisfy homogeneous boundary conditions. In [31], these spaces were enriched conveniently to approximate the boundary integrals that appear in general Green formulas. The resulting derived mimetic operators include an approximation of the boundary conditions. We will not follow this approach here, since the focus of this paper is on mixed-hybrid formulations, which provide another way to incorporate boundary conditions in a numerical scheme.

The duality of the discrete operators helps us to build numerical schemes that satisfy discrete conservation laws. For example, consider the Euler equations in the Lagrangian form:

$$\frac{1}{\rho} \frac{d\rho}{dt} = -\operatorname{div} \mathbf{u}, \quad \rho \frac{d\mathbf{u}}{dt} = -\nabla p, \quad \rho \frac{de}{dt} = -p \operatorname{div} \mathbf{u}, \quad (2.5)$$

where p is the pressure, ρ is the density, \mathbf{u} is the velocity, and e is the internal energy. The system is closed by an equation of state. A mimetic discretization of (2.5) is given by

$$\frac{1}{\rho_h} \frac{d\rho_h}{dt} = -\mathcal{DIV} \mathbf{u}_h, \quad \rho_h \frac{d\mathbf{u}_h}{dt} = -\widetilde{\mathcal{GRAD}} p_h, \quad \rho_h \frac{de_h}{dt} = -p_h \mathcal{DIV} \mathbf{u}_h, \quad (2.6)$$

where p_h , ρ_h , \mathbf{u}_h and e_h are the discrete analogs of the corresponding continuum quantities that appear in (2.5) and \mathcal{DIV} and $\widetilde{\mathcal{GRAD}}$ are the mimetic operators acting, respectively, as divergence and gradient. Let us assume that no external work is done on the system, e.g., $p = 0$ of $\partial\Omega$. The integration by parts and the continuity equation from (2.5) lead to the conservation of the total energy E :

$$\frac{dE}{dt} = \int_{\Omega(t)} \rho \left(\frac{d\mathbf{u}}{dt} \cdot \mathbf{u} + \frac{de}{dt} \right) dx = - \int_{\Omega(t)} (\mathbf{u} \cdot \nabla p + p \operatorname{div} \mathbf{u}) dx = 0. \quad (2.7)$$

To mimic this property, we need the discrete gradient and divergence operators $\widetilde{\mathcal{GRAD}}$ and \mathcal{DIV} to satisfy a discrete integration by parts formula like (2.1). Using the same argument that leads to (2.7), we obtain the conservation of the total discrete energy E_h :

$$\frac{dE_h}{dt} = -[\mathbf{u}_h, \widetilde{\mathcal{GRAD}} p_h]_{\mathcal{F}_h} - [p_h, \mathcal{DIV} \mathbf{u}_h]_{\mathcal{C}_h} = 0.$$

We emphasize that numerical methods that conserve energy usually have other important properties such as correct prediction of a shock position and bounded numerical solution.

Another discretization principle is to derive primary operators that mimic exact identities. This is typically achieved by using the first principles (the divergence and Stokes theorems) to define the primary operators, e.g. (3.7). As the result, we have

$$\mathcal{DIV} \mathcal{CURL} \mathbf{v}_h = 0, \quad \mathcal{CURL} \mathcal{GRAD} p_h = 0 \quad \forall \mathbf{v}_h \in \mathcal{E}_h, \quad \forall p_h \in \mathcal{N}_h.$$

Another consequence of the duality principle is that similar identities hold for the derived mimetic operators. Using the aforementioned explicit formulas for these operators, we immediately obtain that

$$\widetilde{\mathcal{DIV}} \widetilde{\mathcal{CURL}} \mathbf{u}_h = 0, \quad \widetilde{\mathcal{CURL}} \widetilde{\mathcal{GRAD}} q_h = 0 \quad \forall \mathbf{u}_h \in \mathcal{F}_h, \forall q_h \in \mathcal{C}_h.$$

These exact identities allows us to design numerical schemes without non-physical spurious modes. For instance, in the numerical solution of Maxwell's equations, such operators guarantee that the magnetic field \mathbf{B}_h remains divergence-free for all times. Applying the primary divergence operator to a semi-discrete form of Faraday's law of induction, i.e., $\partial \mathbf{B}_h / \partial t = -\mathcal{CURL} \mathbf{E}_h$, we obtain

$$\frac{\partial}{\partial t} (\mathcal{DIV} \mathbf{B}_h) = \mathcal{DIV} \frac{\partial \mathbf{B}_h}{\partial t} = -\mathcal{DIV} \mathcal{CURL} \mathbf{E}_h = 0.$$

Therefore, if \mathbf{B}_h is such that $\mathcal{DIV} \mathbf{B}_h = 0$ at time $t = 0$, this relation will be satisfied at any time $t > 0$.

2.2 Local mimetic operators

From this section, we limit our discussion to elliptic problems and one pair of the primary and derived operators. For the practical implementation of mimetic schemes, it is convenient to write a local integration by parts formula that implies the global one. To do it, we need an additional space Λ_h of pressure unknowns defined typically on mesh faces. Its restriction to cell c is denoted by $\Lambda_{h,c}$ and consists of the vectors $\boldsymbol{\lambda}_c$. We recall that the subscript “ c ” is added to denote the local mimetic operators and the local discrete spaces corresponding to cell c .

Let $\mathcal{DIV}_c: \mathcal{F}_{h,c} \rightarrow \mathcal{C}_{h,c}$ be the primary divergence operator. The derived gradient operator $\widetilde{\mathcal{GRAD}}_c: \mathcal{C}_{h,c} \times \Lambda_{h,c} \rightarrow \mathcal{F}_{h,c}$ satisfies the discrete integration by parts formula

$$\begin{aligned} [\mathcal{DIV}_c \mathbf{u}_c, q_c]_{\mathcal{C}_{h,c}} - [\mathbf{u}_c, \boldsymbol{\lambda}_c]_{\Lambda_{h,c}} &= -[\mathbf{u}_c, \widetilde{\mathcal{GRAD}}_c \begin{pmatrix} q_c \\ \boldsymbol{\lambda}_c \end{pmatrix}]_{\mathcal{F}_{h,c}} \\ \forall \mathbf{u}_c \in \mathcal{F}_{h,c}, \forall q_c \in \mathcal{C}_{h,c}, \forall \boldsymbol{\lambda}_c \in \Lambda_{h,c}, \end{aligned} \quad (2.8)$$

which mimics the continuum Green formula for cell c :

$$\int_c (\operatorname{div} \mathbf{u}) q \, dx - \int_{\partial c} (\mathbf{u} \cdot \mathbf{n}) q \, dx = - \int_c \mathbf{u} \cdot \nabla q \, dx \quad \forall \mathbf{u} \in H_{div}(c), \forall q \in H^1(c).$$

In order to recover formula (2.1) for the global discrete gradient operator, we impose the continuity of $\boldsymbol{\lambda}_c$ and \mathbf{u}_c on the mesh faces, define the local divergence operator as the restriction of the global one, define the local spaces as restrictions of global ones, require that the interface terms cancel each other,

$$\sum_{c \in \Omega_h} [\mathbf{u}_c, \boldsymbol{\lambda}_c]_{\Lambda_{h,c}} = 0, \quad (2.9)$$

and that the local inner products are summed up into global inner products as in (2.3).

The derivation of the mimetic method follows three generic steps. First, we select the degrees of freedom such that the local primary operator, e.g., \mathcal{DTV}_c , has a simple form. Second, we define the inner products in the discrete spaces that satisfy the consistency and stability conditions. Third, we postulate the discrete integration by parts formula and obtain the derived operator, e.g., $\widetilde{\mathcal{GRAD}}_c$, from it. Note that the local derived operator is defined uniquely.

These three steps are discussed in Section 3 for the mixed formulation of the diffusion problem. The flexibility of the mimetic framework is exploited in Section 4.2, where we derive another pair of primary divergence and derived gradient operators for a nonlinear parabolic problem. More examples of mimetic schemes can be found in [9].

2.3 Material properties

The material properties are often included in the definition of the derived mimetic operator. Indeed, the Green formula (2.2) can be rewritten as follows:

$$\int_{\Omega} (\operatorname{div} \mathbf{u}) q \, dx = - \int_{\Omega} \mathbb{K}^{-1} \mathbf{u} \cdot (\mathbb{K} \nabla) q \, dx \quad \forall \mathbf{u} \in H_{div}(\Omega), \forall q \in H_0^1(\Omega). \quad (2.10)$$

According to (2.10), we can define $\widetilde{\mathcal{GRAD}}$ as an approximation of the combined operator $\mathbb{K} \nabla$ and the inner product $[\mathbf{u}_h, \mathbf{v}_h]_{\mathcal{F}_h}$ as an approximation of the right-hand side integral $\int_{\Omega} \mathbb{K}^{-1} \mathbf{u} \cdot \mathbf{v} \, dx$, provided that \mathbf{u}_h and \mathbf{v}_h are the degrees of freedom of \mathbf{u} and \mathbf{v} .

For a perfectly conducting medium, we have the following duality relationship for the first-order curl operators:

$$\int_{\Omega} \operatorname{curl} \mathbf{E} \cdot \mu^{-1} \mathbf{B} \, dx = \int_{\Omega} \varepsilon \mathbf{E} \cdot (\varepsilon^{-1} \operatorname{curl} \mu^{-1} \mathbf{B}) \, dx.$$

In this case the inner products in spaces \mathcal{E}_h and \mathcal{F}_h are the weighted inner products. The weights are the magnetic permeability μ^{-1} and electric permittivity ε . The derived curl operator $\widetilde{\mathcal{CURL}}$ is an approximation of the combined operator $\varepsilon^{-1} \operatorname{curl} \mu^{-1}$.

3 Mixed formulation of diffusion problem

Let $\Omega \in \mathbb{R}^d$ be a polygonal ($d = 2$) or polyhedral ($d = 3$) domain with the Lipschitz continuous boundary. Consider the mixed formulation of the diffusion problem:

$$\begin{aligned} \mathbf{u} &= -\mathbb{K} \nabla p && \text{in } \Omega, \\ \operatorname{div} \mathbf{u} &= b && \text{in } \Omega, \end{aligned} \quad (3.1)$$

subject to the homogeneous Dirichlet boundary conditions on $\partial\Omega$. As usual, we will refer to the scalar unknown as the *pressure* and to the vector unknown as the *flux*. We assume that the diffusion tensor is piecewise constant on mesh Ω_h and we denote its restriction to

cell c by \mathbb{K}_c . If \mathbb{K}_c is not constant on c , we can take its values at the centroids of the mesh cells without losing the approximation order.

In this section, we consider one local mimetic formulation, two FV schemes and two mixed-hybrid FE schemes with the same set of degrees of freedom. Moreover, we consider the schemes that use the same discrete divergence operator and the discrete flux balance equation:

$$\mathbf{u}_c = \mathcal{L}_c(p_c, \boldsymbol{\lambda}_c), \quad \mathcal{DIV}_c \mathbf{u}_c = b_c^I, \quad (3.2)$$

where \mathcal{L}_c is a linear operator and b_c^I is defined later.

3.1 Regular polygonal and polyhedral meshes

The analysis of discretization schemes is typically conducted on a sequence of conformal meshes Ω_h where h is the diameter of the largest cell in Ω_h and $h \rightarrow 0$. A mesh is called conformal if the intersection of any two distinct cells c_1 and c_2 is either empty, or a few mesh points, or a few mesh edges, or a few mesh faces. Cell c is defined as a closed domain in \mathbb{R}^3 (or \mathbb{R}^2) with flat faces and straight edges.

Following [9], we make a few assumptions on the regularity of 3D meshes. Similar assumptions can be derived for 2D meshes by reducing the dimension. Let n_* , ρ_* and γ_* denote various mesh independent constants explained below.

(M1) Every polyhedral cell c has at most n_* faces and each face f has at most n_* edges.

(M2) For every cell c with faces f and edges e , we have

$$\rho_* (\text{diam}(c))^3 \leq |c|, \quad \rho_* (\text{diam}(c))^2 \leq |f|, \quad \rho_* \text{diam}(c) \leq |e|, \quad (3.3)$$

where $|\cdot|$ denotes the Euclidean measure of a mesh object.

(M3) For each cell c , there exists a point \mathbf{x}_c such that c is star-shaped with respect to every point in the sphere of radius $\gamma_* \text{diam}(c)$ centered at \mathbf{x}_c . For each face f , there exists a point $\mathbf{x}_f \in f$ such that f is star-shaped with respect to every point in the disk of radius $\gamma_* \text{diam}(c)$ centered at \mathbf{x}_f as shown in Fig. 2.

(M4) For every cell c , and for every $f \in \partial c$, there exists a pyramid contained in c such that its base equals f , its height equals $\gamma_* \text{diam}(c)$ and the projection of its vertex onto f is \mathbf{x}_f .

The conditions **(M1)**-**(M4)** are sufficient to develop an *a priori* error analysis of various discretization schemes. We recall only two results underpinning this error analysis. The first one is the Agmon inequality that uses **(M4)** and allows us to bound traces of functions:

$$\sum_{f \in \partial c} \|q\|_{L^2(f)}^2 \leq C \left((\text{diam}(c))^{-1} \|q\|_{L^2(c)}^2 + \text{diam}(c) |q|_{H^1(c)}^2 \right) \quad \forall q \in H^1(c). \quad (3.4)$$

The second one is the following approximation result: For any function $q \in H^2(c)$ there exists a polynomial $q^1 \in \mathcal{P}^1(c)$ such that

$$\|q - q^1\|_{L^2(c)} + \text{diam}(c) |q - q^1|_{H^1(c)} \leq C (\text{diam}(c))^2 |q|_{H^2(c)}. \quad (3.5)$$

Hereafter, we will use symbols C , C_1 , C_2 to denote generic constants independent of h .

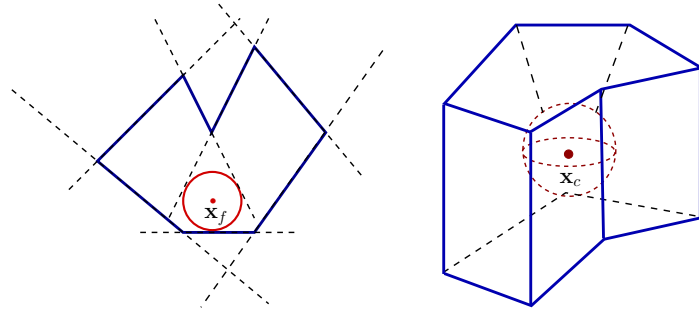


Figure 2: Shape-regular mesh objects.

Remark 3.1 *The mesh regularity assumptions (M1)–(M4) are not unique. They could be generalized to non-star shaped cells [9] by splitting each polygonal or polyhedral cell into the finite number of shape regular simplexes.*

3.2 Mimetic discretization framework

As pointed out at the end of subsection 2.2, the *first step* of the construction of a mimetic scheme consists in the selection of the degrees of freedom. The degrees of freedom are such that the primary divergence operator has a simple form.

The discrete space \mathcal{C}_h consists of one degree of freedom per cell; its dimension equals the number of mesh cells; and for each vector $p_h \in \mathcal{C}_h$ we shall denote the value of p_h associated with cell c by $p_c \in \mathcal{C}_{h,c}$. Furthermore, we denote the vector of degrees of freedom of a smooth function p by $p_h^I \in \mathcal{C}_h$. In the MFD method p_c^I is typically the cell average of p over cell c and this definition is used by the existing superconvergence analysis [14].

The discrete space Λ_h consists of one degree of freedom per mesh face, e.g., λ_f ; its dimension equals the number of mesh faces; and for each vector $\lambda_h \in \Lambda_h$ we shall denote its restriction to cell c by $\lambda_c \in \Lambda_{h,c}$. The continuity of local vectors λ_c across mesh cells is satisfied automatically. The value λ_f can be associated with the value of a smooth function p at the face centroid.

The discrete space \mathcal{F}_h consists of one degree of freedom per boundary face and two degrees of freedom per interior face. For vector $\mathbf{u}_h \in \mathcal{F}_h$, we denote by \mathbf{u}_c its restriction to cell c , and by u_f^c its component associated with face f of cell c . For a smooth function \mathbf{u} , we denote by $\mathbf{u}_h^I \in \mathcal{F}_h$ the vector of degrees of freedom. The value $(u_f^c)^I$ is defined as the integral average of flux $\mathbf{u} \cdot \mathbf{n}_f$ through face f , where \mathbf{n}_f is the face normal fixed once and for all. Hereafter, we consider a subspace of \mathcal{F}_h whose members satisfy the flux continuity constraint

$$u_f^{c_1} = u_f^{c_2} \quad (3.6)$$

on each interior face f shared by cells c_1 and c_2 . With a slight abuse of notation, we shall refer to \mathcal{F}_h as the space that satisfies condition (3.6).

The local primary divergence operator is defined using a straightforward discretization

of the divergence theorem:

$$(\mathcal{DIV}\mathbf{u}_h)|_c \equiv \mathcal{DIV}_c \mathbf{u}_c = \frac{1}{|c|} \sum_{f \in \partial c} |f| \sigma_{c,f} u_f^c, \quad (3.7)$$

where $\sigma_{c,f}$ is either 1 or -1 depending on the mutual orientation of the fixed normal \mathbf{n}_f and the exterior normal $\mathbf{n}_{c,f}$ to ∂c . Observe that this definition remains the same in all coordinate systems.

The *second step* of the construction of a mimetic scheme is to define accurate inner products in $\mathcal{C}_{h,c}$ and $\mathcal{F}_{h,c}$ that satisfy the consistency and stability conditions. The inner product for space $\mathcal{C}_{h,c}$ is simple:

$$[p_c, q_c]_{\mathcal{C}_{h,c}} = |c| p_c q_c. \quad (3.8)$$

Let \mathcal{SC}_c be the space of constant functions. Then, the above inner product implies the obvious result:

$$[p_c^I, q_c^I]_{\mathcal{C}_{h,c}} = \int_c p q \, dx \quad \forall p \in \mathcal{P}^0(c), \quad \forall q \in \mathcal{SC}_c.$$

Despite its simplicity, we can use this relation to formulate the general principle that we apply to the derivation of other inner products. We define the consistency condition as the following exactness property: *the L^2 inner product of two smooth functions is equal to the mimetic inner product of their interpolants when one of the functions (p in this case) is a polynomial of a given degree and the other one belongs to a sufficiently rich space (possibly infinite dimensional) that must include polynomial functions.*

The exactness property implies that L^2 inner products of a large class of functions can be calculated exactly using the degrees of freedom. In particular, we write the consistency condition for the inner product on space $\mathcal{F}_{h,c}$ as the exactness property:

$$[\mathbf{u}_c^I, \mathbf{v}_c^I]_{\mathcal{F}_{h,c}} = \int_c \mathbb{K}_c^{-1} \mathbf{u} \cdot \mathbf{v} \, dx \quad \forall \mathbf{u} \in (\mathcal{P}^0(c))^d, \quad \forall \mathbf{v} \in \mathcal{SF}_c, \quad (3.9)$$

where \mathcal{SF}_c is a specially designed space containing the constant vector-functions:

$$\mathcal{SF}_c = \{ \mathbf{v} : \operatorname{div} \mathbf{v} \in \mathcal{P}^0(c), \quad \mathbf{v} \cdot \mathbf{n}_f \in \mathcal{P}^0(f) \quad \forall f \in \partial c \}$$

Let us show that the right-hand side of (3.9) can be calculated using the degrees of freedom. Let q^1 be a linear function such that $\mathbb{K}_c \nabla q^1 = \mathbf{u}$. Inserting \mathbf{u} in (3.9), integrating by parts, and using the properties of \mathcal{SF}_c , we obtain

$$\int_c \nabla q^1 \cdot \mathbf{v} \, dx = - \int_c (\operatorname{div} \mathbf{v}) q^1 \, dx + \int_{\partial c} (\mathbf{v} \cdot \mathbf{n}) q^1 \, dx = \sum_{f \in \partial c} \mathbf{v} \cdot \mathbf{n}_{c,f} \left(\int_f q^1 \, dx - \frac{|f|}{|c|} \int_c q^1 \, dx \right).$$

Let $\mathbf{M}_{\mathcal{F},c}$ be the inner product matrix and $\mathbf{r}_c(q^1) \in \mathcal{F}_{h,c}$ be the vector with components $\sigma_{c,f} \left(\int_f q^1 \, dx - \frac{|f|}{|c|} \int_c q^1 \, dx \right)$. Then, combining the last formulas, we have

$$\begin{aligned} [(\mathbb{K}_c \nabla q^1)_c^I, \mathbf{v}_c^I]_{\mathcal{F}_{h,c}} &= ((\mathbb{K}_c \nabla q^1)_c^I)^T \mathbf{M}_{\mathcal{F},c} \mathbf{v}_c^I = \sum_{f \in \partial c} \mathbf{v} \cdot \mathbf{n}_f \sigma_{c,f} \left(\int_f q^1 \, dx - \frac{|f|}{|c|} \int_c q^1 \, dx \right) \\ &= (\mathbf{r}_c(q^1))^T \mathbf{v}_c^I. \end{aligned}$$

Since \mathbf{v} is any function in \mathcal{SF}_c , we can show that its interpolant \mathbf{v}_c^I is any vector in $\mathcal{F}_{h,c}$. Indeed, it is sufficient to define a few functions \mathbf{v} as the solutions of cell-based PDEs with different boundary conditions. Hence, the consistency condition gives us the following matrix equations

$$\mathbf{M}_{\mathcal{F},c}(\mathbb{K}_c \nabla q^1)_c^I = \mathbf{r}_c(q^1) \quad \forall q^1 \in \mathcal{P}^1(c). \quad (3.10)$$

Due to the linearity of these equations, it is sufficient to consider only three (two in two dimensions) linearly independent linear functions: $q_x^1 = x$, $q_y^1 = y$, and $q_z^1 = z$. Let

$$\mathbf{N}_c = [(\mathbb{K}_c \nabla x)_c^I \ (\mathbb{K}_c \nabla y)_c^I \ (\mathbb{K}_c \nabla z)_c^I], \quad \mathbf{R}_c = [\mathbf{r}_c(x) \ \mathbf{r}_c(y) \ \mathbf{r}_c(z)] \quad (3.11)$$

be two rectangular $n_c \times 3$ matrices where n_c is the number of faces in cell c . The equations (3.10) are now equivalent to the matrix equation:

$$\mathbf{M}_{\mathcal{F},c} \mathbf{N}_c = \mathbf{R}_c. \quad (3.12)$$

Note that a symmetric positive definite solution $\mathbf{M}_{\mathcal{F},c}$ (if it exists) is not unique even for a tetrahedral cell c . The existence of solutions is based on the following result proved in [9].

Lemma 3.1 *Let matrices \mathbf{N}_c and \mathbf{R}_c be defined as in (3.11). Then, $\mathbf{R}_c^T \mathbf{N}_c = |c| \mathbb{K}_c$.*

This lemma allows us to write the explicit formula for matrix $\mathbf{M}_{\mathcal{F},c}$:

$$\mathbf{M}_{\mathcal{F},c} = \mathbf{R}_c(\mathbf{R}_c^T \mathbf{N}_c)^{-1} \mathbf{R}_c^T + \gamma_c \mathbf{P}_c, \quad \mathbf{P}_c = \mathbf{I} - \mathbf{N}_c(\mathbf{N}_c^T \mathbf{N}_c)^{-1} \mathbf{N}_c^T$$

with a positive factor γ_c in front of the projection matrix \mathbf{P}_c . A recommended choice for γ_c is the mean trace of the first term. A family of mimetic schemes is obtained if we replace γ_c by an arbitrarily symmetric positive definite matrix \mathbf{G}_c :

$$\mathbf{M}_{\mathcal{F},c} = \mathbf{R}_c(\mathbf{R}_c^T \mathbf{N}_c)^{-1} \mathbf{R}_c^T + \mathbf{P}_c \mathbf{G}_c \mathbf{P}_c. \quad (3.13)$$

The stability of the resulting mimetic method depends on the spectral bounds of matrix \mathbf{G}_c which should be uniformly bounded by γ_c . Algebraically, it means that there exists two generic constants C_1 and C_2 such that

$$C_1 |c| \sum_{f \in \partial c} |v_f^c|^2 \leq \mathbf{v}_c^T \mathbf{M}_{\mathcal{F},c} \mathbf{v}_c^T \leq C_2 |c| \sum_{f \in \partial c} |v_f^c|^2 \quad (3.14)$$

holds for every $\mathbf{v}_c = \{v_f^c\}_{f \in \partial c}$. This formula is called the *stability condition* in the mimetic discretization framework. The existence of the mesh independent constants C_1 and C_2 can be shown using assumptions **(M1)**-**(M4)**.

The *third* step of the construction of a mimetic scheme is to postulate either the local or global integration by parts formula and derive the gradient operator from it. For instance, given the global discrete operators $\mathcal{DIV}: \mathcal{F}_h \rightarrow \mathcal{C}_h$ and $\widetilde{\mathcal{GRAD}}: \mathcal{C}_h \rightarrow \mathcal{F}_h$, we can write the mimetic scheme as follows: Find $\mathbf{u}_h \in \mathcal{F}_h$ and $p_h \in \mathcal{C}_h$ such that

$$\mathbf{u}_h = -\widetilde{\mathcal{GRAD}} p_h, \quad \mathcal{DIV} \mathbf{u}_h = b^I,$$

where $b^I \in C_h$.

The local mimetic formulation requires us to define $[\mathbf{u}_c, \boldsymbol{\lambda}_c]_{\Lambda_{h,c}}$ which satisfies condition (2.9). Let

$$[\mathbf{u}_c, \boldsymbol{\lambda}_c]_{\Lambda_{h,c}} = \sum_{f \in \partial c} \sigma_{c,f} |f| \lambda_f u_f^c. \quad (3.15)$$

Then, the local formulation is to find $\mathbf{u}_c \in \mathcal{F}_{h,c}$ and $p_c \in \mathcal{C}_{h,c}$ in all mesh cells such that

$$\mathbf{u}_c = -\widetilde{\mathcal{GRAD}}_c \begin{pmatrix} p_c \\ \boldsymbol{\lambda}_c \end{pmatrix}, \quad \mathcal{DIV}_c \mathbf{u}_c = b_c^I$$

subject to the flux continuity conditions (3.6) and the homogeneous Dirichlet boundary conditions $\lambda_f = 0$ for $f \in \partial\Omega$. The local derived operator has the explicit form:

$$\widetilde{\mathcal{GRAD}}_c \begin{pmatrix} p_c \\ \boldsymbol{\lambda}_c \end{pmatrix} = -\mathbf{M}_{\mathcal{F},c}^{-1} \begin{pmatrix} \sigma_{c,f_1} |f_1| (p_c - \lambda_{f_1}) \\ \vdots \\ \sigma_{c,f_{n_c}} |f_{n_c}| (p_c - \lambda_{f_{n_c}}) \end{pmatrix}. \quad (3.16)$$

Lemma 3.2 *Under assumption (2.3) the local and global mimetic formulations are equivalent.*

Proof. Let \mathbf{v}_h be an arbitrary vector in \mathcal{F}_h and \mathbf{v}_c be its restriction to cell c . To show that the solution to the local mimetic formulation is the solution to the global one, we first multiply both sides of the local constitutive equations by \mathbf{v}_c , then sum up the results over the mesh cells, cancel all internal face terms containing λ_f , and finally use the local duality relation (2.8) between \mathcal{DIV}_c and $\widetilde{\mathcal{GRAD}}_c$ to obtain:

$$\sum_c [\mathbf{u}_c, \mathbf{v}_c]_{\mathcal{F}_{h,c}} = - \sum_c [\widetilde{\mathcal{GRAD}}_c \begin{pmatrix} p_c \\ \boldsymbol{\lambda}_c \end{pmatrix}, \mathbf{v}_c]_{\mathcal{F}_{h,c}} = \sum_c [\mathcal{DIV}_c \mathbf{v}_c, p_c]_{\mathcal{C}_{h,c}}.$$

From the additivity of the inner products and (2.1) we obtain that

$$[\mathbf{u}_h, \mathbf{v}_h]_{\mathcal{F}_h} = [\mathcal{DIV} \mathbf{v}_h, p_h]_{\mathcal{C}_h} = -[\widetilde{\mathcal{GRAD}} p_h, \mathbf{v}_h]_{\mathcal{F}_h} \quad \forall \mathbf{v}_h \in \mathcal{F}_h,$$

which implies that $\mathbf{u}_h = -\widetilde{\mathcal{GRAD}} p_h$.

To show the opposite statement, we repeat the above argument in the reverse order. This proves the assertion of the lemma. \square

Let us consider the matrix equation $\mathbf{N}_c = \mathbf{W}_{\mathcal{F},c} \mathbf{R}_c$ (compare with (3.12)). To implement the mimetic scheme in a computer program, we need to know only matrix $\mathbf{W}_{\mathcal{F},c}$. The general solution to the matrix equation is

$$\mathbf{W}_{\mathcal{F},c} = \mathbf{N}_c (\mathbf{N}_c^T \mathbf{R}_c)^{-1} \mathbf{N}_c^T + \widetilde{\mathbf{G}}_c (\mathbf{I} - \mathbf{R}_c (\mathbf{R}_c^T \mathbf{R}_c)^{-1} \mathbf{R}_c^T),$$

where $\widetilde{\mathbf{G}}_c$ is an arbitrary $n_c \times n_c$ matrix, possibly non-symmetric. This formula leads to a large family of stable and unstable schemes that we refer to as the *extended mixed-hybrid family* of schemes. Positive definiteness of $\mathbf{W}_{\mathcal{F},c}$ is necessary for proving the scheme's convergence following the path described in [37].

If in addition $\mathbf{W}_{\mathcal{F},c}$ is symmetric, then it is one of the matrices $\mathbf{M}_{\mathcal{F},c}^{-1}$. The classical two-point flux FV scheme is obtained when all matrices $\mathbf{W}_{\mathcal{F},c}$ are positive definite and diagonal.

3.2.1 Error estimates

Let Ω have a Lipschitz continuous boundary. Furthermore, let every cell c be shape regular as explained in Sec. 3.1. We assume that \mathbf{x}_c is the centroid of cell c . We use the triple-bar notation, e.g., $||| \cdot |||$, for the norms induced by the mimetic inner products. Then, the interpolants of the exact solution, $p^I \in \mathcal{C}_h$ and $\mathbf{u}^I \in \mathcal{F}_h$, satisfy [14]

$$|||p^I - p_h|||_{\mathcal{C}_h} + |||\mathbf{u}^I - \mathbf{u}_h|||_{\mathcal{F}_h} \leq C h,$$

where p_h and \mathbf{u}_h are solutions of the global mimetic formulation. If in addition Ω is convex and C_1 in (3.14) is sufficiently large, then

$$|||p^I - p_h|||_{\mathcal{C}_h} \leq C h^2.$$

3.3 Finite volume discretization framework

Two examples of FV schemes that fit within the mimetic framework are the mixed finite volume (MFV) method [25] and the hybrid finite volume (HFV) method [29]. Both methods give a family of schemes because a stabilization term, which can be suitably parameterized, appears in their formulation. Their design principles are based on conditions that imply the mimetic duality principle.

Both methods use the same degrees of freedom for pressure and flux as the local mimetic formulation and the same discrete flux balance equation, i.e., $\mathcal{DIV}_c \mathbf{u}_c = b_c^I$. Recall that \mathbf{u}_c collects the flux unknowns associated with cell c . The local pressure unknowns are the cell pressure p_c , which is associated with the interior of c , and the interface pressure λ_f , which is associated with face f . In the formulation of these FV methods, p_c can be associated with the pressure value at any point inside the cell. As in the previous subsection, $\boldsymbol{\lambda}_c = \{\lambda_f\}_{f \in \partial c}$ is the vector whose size is equal to the number of faces in cell c .

In the HFV method, a discrete gradient in cell c is defined by applying the mid-point quadrature rule to the divergence theorem:

$$\nabla_c \begin{pmatrix} p_c \\ \boldsymbol{\lambda}_c \end{pmatrix} = \frac{1}{|c|} \sum_{f \in \partial c} |f| \lambda_f \mathbf{n}_{c,f} = \frac{1}{|c|} \sum_{f \in \partial c} |f| (\lambda_f - p_c) \mathbf{n}_{c,f}. \quad (3.17)$$

This formula provides the exact value of the gradient whenever p is a linear function since for any constant vector \mathbf{a} and any position vector \mathbf{x}_c , we have the geometric identity

$$|c| \mathbf{a} = \sum_{f \in \partial c} |f| \mathbf{a} \cdot (\mathbf{x}_f - \mathbf{x}_c) \mathbf{n}_{c,f},$$

where \mathbf{x}_f is the face centroid.

Formula (3.17) is used to define the numerical scheme after an additional *stabilization term* $\mathbf{s}_{c,f}$, is included in the definition of the numerical flux u_f^c :

$$u_f^c = -\mathbf{n}_f \cdot \mathbb{K}_c \nabla_c \begin{pmatrix} p_c \\ \boldsymbol{\lambda}_c \end{pmatrix} + \mathbf{s}_{c,f}. \quad (3.18)$$

Like in the mimetic framework, the stabilization term is designed very carefully to preserve the consistency of the scheme. Let \mathbf{F}_c be the diagonal matrix with entries $|f|$ on the main diagonal, $f \in \partial c$. Similarly, let Σ_c be the diagonal matrix with entries $\sigma_{c,f}$. Furthermore, let $\mathbb{1}^T = (1, 1, \dots, 1)^T$, and

$$S_{c,f}(p_c, \boldsymbol{\lambda}_c) = \lambda_f - p_c - \nabla_c \begin{pmatrix} p_c \\ \boldsymbol{\lambda}_c \end{pmatrix} \cdot (\mathbf{x}_f - \mathbf{x}_c).$$

Note that the last expression is zero on linear pressure functions. The numerical flux is defined implicitly as the solution of

$$(\tilde{p}_c \mathbb{1} - \tilde{\boldsymbol{\lambda}}_c)^T \Sigma_c \mathbf{F}_c \mathbf{u}_c = |c| \mathbb{K}_c \nabla_c \begin{pmatrix} p_c \\ \boldsymbol{\lambda}_c \end{pmatrix} \cdot \nabla_c \begin{pmatrix} \tilde{p}_c \\ \tilde{\boldsymbol{\lambda}}_c \end{pmatrix} + \sum_{f \in \partial c} \alpha_{c,f} \frac{|f|}{d_{c,f}} S_{c,f}(p_c, \boldsymbol{\lambda}_c) S_{c,f}(\tilde{p}_c, \tilde{\boldsymbol{\lambda}}_c) \quad (3.19)$$

for any \tilde{p}_c and $\tilde{\boldsymbol{\lambda}}_c$. Here $\alpha_{c,f}$ is a positive parameter and $d_{c,f}$ is the distance between \mathbf{x}_c and the plane containing face f . After a few algebraic manipulations, we obtain:

$$\mathbf{s}_{c,f} = \sigma_{c,f} \sum_{f' \in \partial c} \alpha_{cf'} \frac{|f'|}{d_{cf'}} S_{cf'}(p_c, \boldsymbol{\lambda}_c) \left[-\frac{\delta_{f,f'}}{|f|} + \frac{1}{|c|} \mathbf{n}_{c,f} \cdot (\mathbf{x}_{f'} - \mathbf{x}_c) \right]$$

where $\delta_{f,f'}$ is the Kronecker symbol. It is obvious that the stabilization term is zero when it is calculated using the degrees of freedom of a linear function.

The right-hand side of (3.19) is a symmetric bilinear form with respect to the pressure unknowns. It is positive definite when $\alpha_{c,f} > 0$ and $\lambda_f = 0$ on $f \in \partial \Omega$. It is uniformly bounded from below when $\alpha_{c,f}$ are sufficiently large and the mesh satisfies the regularity conditions described in Section 3.1.

Remark 3.2 Equation (3.19) is the key design principle. When p_c is associated with the cell centroid, the left-hand side of this equation coincides with the left-hand side of (2.8) where the divergence is given by (3.7) and the interface term is defined by (3.15). So, equation (3.19) is also a representation of the duality principle.

Formula (3.17) can be rewritten using the mimetic matrix \mathbf{N}_c as follows:

$$\nabla_c^{HFV} \begin{pmatrix} p_c \\ \boldsymbol{\lambda}_c \end{pmatrix} = \frac{\mathbb{K}_c^{-1}}{|c|} \mathbf{N}_c^T \mathbf{F}_c \boldsymbol{\lambda}_c.$$

This formula should be compared with the formula for the discrete gradient in the MFV method:

$$\nabla_c^{MFV} \begin{pmatrix} p_c \\ \boldsymbol{\lambda}_c \end{pmatrix} = -\frac{\mathbb{K}_c^{-1}}{|c|} \mathbf{R}_c^T \Sigma_c \mathbf{u}_c.$$

This formula is exact for a linear pressure function and constant flux, but it also has to be stabilized. The vector of numerical fluxes \mathbf{u}_c is defined as the solution of

$$(\mathbf{v}_c)^T \mathbf{G}_c \mathbf{u}_c = (p_c \mathbb{1} - \boldsymbol{\lambda}_c)^T \Sigma_c \mathbf{F}_c \mathbf{v}_c \quad \forall \mathbf{v}_c \in \mathcal{F}_{h,c} \quad (3.20)$$

where \mathbf{G}_c is a symmetric positive definite matrix. This design principle shows even clear connection with the mimetic duality principle (2.8). Since \mathbf{G}_c is invertible, we have that \mathbf{u}_c is a linear combination of p_c and $\boldsymbol{\lambda}_c$, i.e. condition (3.2). We can summarize the above discussions in the following lemma.

Lemma 3.3 *Any linearity preserving mixed-hybrid scheme of type (3.2) with the degrees of freedom given by \mathcal{C}_h , Λ_h , and \mathcal{F}_h is a member of the extended mixed-hybrid family of schemes. In addition, let $\mathbf{u}_c = \mathcal{L}_c(p_c, \boldsymbol{\lambda}_c)$ and assume that the bilinear form*

$$\mathcal{B}((\tilde{p}_c, \tilde{\boldsymbol{\lambda}}_c), (p_c, \boldsymbol{\lambda}_c)) := (\tilde{p}_c \mathbb{1} - \tilde{\boldsymbol{\lambda}}_c)^T \Sigma_c \mathbf{F}_c \mathcal{L}(p_c, \boldsymbol{\lambda}_c) \quad (3.21)$$

is symmetric, uniformly coercive and uniformly bounded (with respect to some norm that may depend on the problem). Then, the resulting scheme belongs to the mimetic family of schemes.

Proof. The most general form of the constitutive equation in (3.2) is given by the linear relationship

$$\mathbf{u}_c = \mathcal{L}_c(p_c, \boldsymbol{\lambda}_c) = -\tilde{\mathbf{W}}_{\mathcal{F},c} \begin{pmatrix} \boldsymbol{\lambda}_c \\ p_c \end{pmatrix}$$

with a rectangular $n_c \times (n_c + 1)$ matrix $\tilde{\mathbf{W}}_{\mathcal{F},c} = [\tilde{\mathbf{W}}_{\mathcal{F},c}^{(1)}, \tilde{\mathbf{W}}_{\mathcal{F},c}^{(2)}]$. Since the scheme is exact for constant pressure functions, we have

$$0 = -\tilde{\mathbf{W}}_{\mathcal{F},c} \begin{pmatrix} \mathbb{1} \\ 1 \end{pmatrix}.$$

Multiplying the last equation by p_c and subtracting from the previous one, we obtain

$$\mathbf{u}_c = \tilde{\mathbf{W}}_{\mathcal{F},c}^{(1)}(p_c \mathbb{1} - \boldsymbol{\lambda}_c).$$

By our assumption, this formula is exact for all linear pressure functions and the corresponding constant flux functions. Let us take linearly independent pressure functions x , y , z and use the matrix notations introduced above to derive the following consequence of the linearity preservation property:

$$\mathbf{N}_c = \tilde{\mathbf{W}}_{\mathcal{F},c}^{(1)} \Sigma_c \mathbf{F}_c^{-1} \mathbf{R}_c.$$

Hence, $\tilde{\mathbf{W}}_{\mathcal{F},c}^{(1)} = \mathbf{W}_{\mathcal{F},c} \mathbf{F}_c \Sigma_c$ and the resulting scheme belongs to the extended mixed-hybrid family of schemes. Now

$$(\tilde{p}_c \mathbb{1} - \tilde{\boldsymbol{\lambda}}_c)^T \Sigma_c \mathbf{F}_c \mathbf{u}_c = (\tilde{p}_c \mathbb{1} - \tilde{\boldsymbol{\lambda}}_c)^T \Sigma_c \mathbf{F}_c \mathbf{W}_{\mathcal{F},c} \mathbf{F}_c \Sigma_c (p_c \mathbb{1} - \boldsymbol{\lambda}_c).$$

Our symmetry and coercivity assumptions imply that $\mathbf{W}_{\mathcal{F},c}$ is symmetric and positive definite; hence, it is invertible and $\mathbf{W}_{\mathcal{F},c}^{-1}$ coincides with one of the mimetic inner product matrices $\mathbf{M}_{\mathcal{F},c}$. Let $\tilde{\mathbf{u}}_c = \mathbf{W}_{\mathcal{F},c}^{(1)}(\tilde{p}_c \mathbb{1} - \tilde{\boldsymbol{\lambda}}_c)$. Then,

$$(\tilde{p}_c \mathbb{1} - \tilde{\boldsymbol{\lambda}}_c)^T \Sigma_c \mathbf{F}_c \mathbf{u}_c = \tilde{\mathbf{u}}_c^T \mathbf{W}_{\mathcal{F},c}^{-1} \mathbf{u}_c.$$

The uniform coercivity and boundness conditions imply that matrix $\mathbf{W}_{\mathcal{F},c}^{-1}$ satisfies the mimetic stability condition. This proves the assertion of the lemma. \square

A detailed comparison of MFD, HFV and MFV methods is performed in [26]. In particular, the authors have shown that all schemes can be generalized to provide the identical families of numerical schemes.

3.4 Finite element discretization framework

3.4.1 Raviart-Thomas FE method on simplexes

Let us consider the family of mimetic schemes, where the mass matrix is given in the form of equation (3.13). When the mesh is formed by simplexes, e.g., triangles in 2D and tetrahedra in 3D, there is a choice of the stabilization matrix $\mathbf{P}_c \mathbf{G}_c \mathbf{P}_c$ that provides the mass matrix from the lowest order Raviart-Thomas space [16]. For a simplex, the stabilization matrix is a one-rank matrix, $\mathbf{P}_c \mathbf{G}_c \mathbf{P}_c = \mathbf{p}_c^T [g_c] \mathbf{p}_c$, where

$$g_c = \frac{1}{d^2(d+1)} \sum_{f \in \partial c} (\mathbf{x}_f - \mathbf{x}_c)^T \mathbb{K}_c^{-1} (\mathbf{x}_f - \mathbf{x}_c)$$

and vector $\mathbf{p}_c^T = (|f_1|, |f_2|, \dots, |f_{d+1}|)$, $f_i \in \partial c$.

3.4.2 Virtual element method

The VEM was originally introduced as an evolution of the MFD method. In the classical finite element spirit, the duality principle is now incorporated in the weak formulation: *Find $\mathbf{u}_h \in \widetilde{\mathcal{SF}}_h$ and $p_h \in \widetilde{\mathcal{C}}_h$ such that*

$$a_h(\mathbf{u}_h, \mathbf{v}_h) - (\operatorname{div}_h \mathbf{v}_h, p_h)_{L^2(\Omega)} = 0 \quad \forall \mathbf{v}_h \in \widetilde{\mathcal{SF}}_h, \quad (3.22a)$$

$$(\operatorname{div}_h \mathbf{u}_h, q_h)_{L^2(\Omega)} = (b, q_h)_{L^2(\Omega)} \quad \forall q_h \in \widetilde{\mathcal{C}}_h, \quad (3.22b)$$

where $\widetilde{\mathcal{C}}_h$ is the space of piecewise constant functions isometric to \mathcal{C}_h , $\widetilde{\mathcal{SF}}_h$ is a virtual space built from the local virtual spaces $\widetilde{\mathcal{SF}}_c$,

$$a_h(\mathbf{u}_h, \mathbf{v}_h) = \sum_{c \in \Omega_h} a_{h,c}(\mathbf{u}_h, \mathbf{v}_h), \quad a_{h,c}(\mathbf{u}_h, \mathbf{v}_h) = a_{h,c}^{(1)}(\mathbf{u}_h, \mathbf{v}_h) + a_{h,c}^{(2)}(\mathbf{u}_h, \mathbf{v}_h),$$

$a_{h,c}^{(1)}$ and $a_{h,c}^{(2)}$ are the consistency and stability terms (to be defined later in the section), and operator div_h is defined cell-by-cell as the local L^2 -orthogonal projection of the continuum divergence operator onto $\widetilde{\mathcal{C}}_h$. The virtual space $\widetilde{\mathcal{SF}}_c$ includes polynomial as well as non-polynomial functions.

A new design principle is given by the unisolvency property. The virtual space $\widetilde{\mathcal{SF}}_c$ is built to be isomorphic to the mimetic space $\mathcal{F}_{h,c}$, i.e., the space of degrees of freedom. The virtual space is defined as the subspace of \mathcal{SF}_c :

$$\widetilde{\mathcal{SF}}_c = \{ \mathbf{v} : \operatorname{div} \mathbf{v} \in \mathcal{P}^0(c), \quad \mathbf{v} \cdot \mathbf{n}_f \in \mathcal{P}^0(f) \quad \forall f \in \partial c, \quad \operatorname{curl} \mathbf{v} = 0 \}.$$

In order to describe the splitting of the bilinear form $a_{h,c}(\mathbf{u}_h, \mathbf{v}_h)$ we need to introduce the problem-dependent L^2 projector $\Pi_c : \widetilde{\mathcal{SF}}_c \rightarrow (\mathcal{P}^0(c))^d$:

$$a(\mathbf{v} - \Pi_c(\mathbf{v}), \mathbf{v}^0) = 0 \quad \forall \mathbf{v}^0 \in (\mathcal{P}^0(c))^d,$$

where $a(\mathbf{v}, \mathbf{u}) = (\mathbb{K}_c^{-1} \mathbf{v}, \mathbf{u})_{L^2(c)}$. The projector is computable using only the degrees of freedom [13]. We define the consistency term as

$$a_{h,c}^{(1)}(\mathbf{u}_h, \mathbf{v}_h) = a(\Pi_c(\mathbf{u}_h), \Pi_c(\mathbf{v}_h)) = \int_c \mathbb{K}_c^{-1} \Pi_c(\mathbf{u}_h) \cdot \Pi_c(\mathbf{v}_h) dx,$$

and the stability term as

$$a_{h,c}^{(2)}(\mathbf{u}_h, \mathbf{v}_h) = (\mathbf{u}_h - \Pi_c(\mathbf{u}_h), \mathbf{v}_h - \Pi_c(\mathbf{v}_h))_{L^2(c)}.$$

To generate a family of schemes, we can replace the L^2 inner product with any other spectrally equivalent bilinear form. Like in the mimetic framework, the consistency term is the exactness property that holds when the first argument in the bilinear form is the constant function:

$$a_{h,c}^{(1)}(\mathbf{u}_h, \mathbf{v}_h) = \int_c \mathbb{K}_c^{-1} \Pi_c(\mathbf{u}_h) \cdot \Pi_c(\mathbf{v}_h) dx = \int_c \mathbb{K}_c^{-1} \Pi_c(\mathbf{u}_h) \cdot \mathbf{v}_h dx \quad \forall \mathbf{v}_h \in \widetilde{\mathcal{SF}}_h.$$

Hence, the contribution of this term to the local mass matrix is like in the mimetic scheme, $\mathbf{R}_c (\mathbf{R}_c^T \mathbf{N}_c)^{-1} \mathbf{R}_c^T$.

The conventional FE hybridization procedure works for the VEM as well. The first equation in the variational formulation is replaced by a set of cell-based equations:

$$a_{h,c}(\mathbf{u}_{h,c}, \mathbf{v}_{h,c}) - (\operatorname{div}_{h,c} \mathbf{v}_{h,c}, p_h)_{L^2(c)} + \langle \mathbf{v}_{h,c} \cdot \mathbf{n}, \lambda_h \rangle_{\partial c} = 0, \quad (3.23)$$

where $\mathbf{u}_{h,c}, \mathbf{v}_{h,c} \in \widetilde{\mathcal{SF}}_c$, div_c is the restriction of div_h to cell c , and λ_h is the Lagrange multiplier. It also holds that $\operatorname{div}_{h,c} \mathbf{v}_{h,c} = \mathcal{DIV}_c \mathbf{v}_c$ and

$$\langle \mathbf{v}_{h,c} \cdot \mathbf{n}, \lambda_h \rangle_{\partial c} = \sum_{f \in \partial c} \sigma_{c,f} |f| v_f^c \lambda_f,$$

where λ_f is the constant value of the Lagrange multiplier on face f (compare with (3.15)). The continuity equation is algebraically equivalent to (3.6). Introducing vector $\boldsymbol{\lambda}_c = \{\lambda_f\}_{f \in \partial c}$ and recalling that p_h has the constant value p_c over cell c , the hybridized equation can be rewritten as follows:

$$(p_c \mathbb{1} - \boldsymbol{\lambda}_c)^T \Sigma_c \mathbf{F}_c \mathbf{v}_c = a_{h,c}^{(1)}(\mathbf{u}_h, \mathbf{v}_h),$$

which also provides the relation $\mathbf{u}_c = \mathcal{L}(p_c, \boldsymbol{\lambda}_c)$. The VEM is the linearity-preserving method. According to Lemma 3.3, the lowest-order mixed-hybrid virtual element scheme is a member of the mimetic family of schemes.

4 Recent developments of the mimetic framework

We highlight the new developments that extend the value of the mimetic framework for various physical applications.

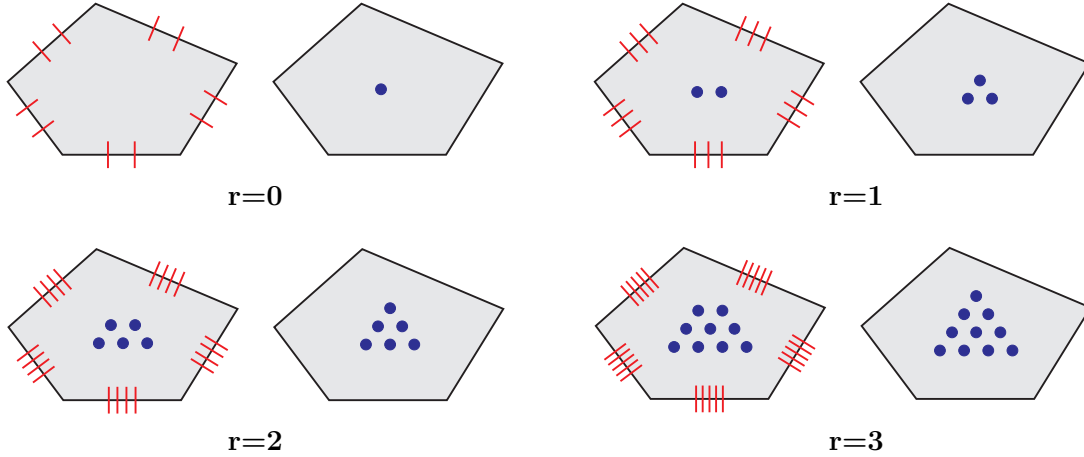


Figure 3: Degrees of freedom for $0 \leq r \leq 3$ on a polygonal cell; for each polynomial degree r we show the flux degrees of freedom on the left and the scalar degrees of freedom on the right. The edge/face moments of the normal component of the flux are denoted by a vertical line; the cell moments are denoted by a bullet.

4.1 High-order schemes

The development of a high-order mimetic scheme follows the same three steps described above for the low-order mimetic schemes. In the first step, we select the degrees of freedom that are convenient for the definition of the primary divergence operator, still denoted by \mathcal{DIV} . With a slight abuse of notation we still use the symbols \mathcal{C}_h and \mathcal{F}_h for the discrete spaces of pressure and flux unknowns, respectively.

The discrete space \mathcal{C}_h contains multiple pressure unknowns that can be associated with the solution moments up to order r . The discrete space \mathcal{F}_h contains multiple flux unknowns both associated with the mesh cells and the mesh faces. The cell-based degrees of freedom represent moments of the flux up to order r except for the zero-th order moment. The face-based degrees of freedom represent flux moments up to order $r + 1$, see Fig. 3.

The discrete divergence operator $\mathcal{DIV}: \mathcal{F}_h \rightarrow \mathcal{C}_h$ is defined cell-wise from the commutation property:

$$(\mathcal{DIV} \mathbf{u}^I)_c = \mathcal{DIV}_c \mathbf{u}_c^I = (\operatorname{div} \mathbf{u})_c^I,$$

which is also a useful property for the error analysis. This is the new design principle that can be generalized to other mimetic operators. The right-hand side is computable using only the degrees of freedom of \mathbf{u}^I . Let $\psi \in \mathcal{P}^r(c)$ be a polynomial of order at most r . Then, the definition of the moment and integration by parts give

$$(\operatorname{div} \mathbf{u})_c^I = \frac{1}{|c|} \int_c (\operatorname{div} \mathbf{u}) \psi \, dx = - \int_c \mathbf{u} \cdot \nabla \psi \, dx + \sum_{f \in \partial c} \int_f (\mathbf{u} \cdot \mathbf{n}_{c,f}) \psi \, dx.$$

In the second step, we define the mimetic inner products in spaces \mathcal{C}_h and \mathcal{F}_h as accurate approximations of the L^2 inner products of pressure and flux functions. The derivation is

based on two high-order consistency conditions. Since the local space $\mathcal{C}_{h,c}$ is isomorphic to $\mathcal{P}^r(c)$, the first consistency condition is the obvious generalization of (3.8):

$$[p_c^I, q_c^I]_{\mathcal{C}_{h,c}} = \int_c p q \, dx \quad \forall p \in \mathcal{P}^r(c), \forall q \in \mathcal{P}^r(c).$$

The consistency condition in space $\mathcal{F}_{h,c}$ is defined as the following exactness property:

$$[\mathbf{u}_c^I, \mathbf{v}_c^I]_{\mathcal{F}_{h,c}} = \int_c \mathbb{K}_c^{-1} \mathbf{u} \cdot \mathbf{v} \, dx \quad \forall \mathbf{u} \in \mathbb{K}_c \nabla \mathcal{P}^{r+2}(c), \forall \mathbf{v} \in \mathcal{SF}_c,$$

where \mathcal{SF}_c is a specially designed space containing the vector functions $(\mathcal{P}^{r+1}(c))^d$:

$$\mathcal{SF}_c = \{ \mathbf{v} : \operatorname{div} \mathbf{v} \in \mathcal{P}^r(c), \quad \mathbf{v} \cdot \mathbf{n}_f \in \mathcal{P}^{r+1}(f) \quad \forall f \in \partial c \}.$$

It is easy to show that the right-hand side of the consistency condition is computable using the degrees of freedom introduced above. Let $q \in \mathcal{P}^{r+2}(c)$ be such that $\mathbf{u} = \mathbb{K}_c \nabla q$. Then,

$$\int_c \mathbb{K}_c^{-1} \mathbf{u} \cdot \mathbf{v} \, dx = - \int_c (\operatorname{div} \mathbf{v}) q \, dx + \sum_{f \in \partial c} \int_f (\mathbf{v} \cdot \mathbf{n}_{c,f}) q \, dx.$$

As \mathbf{v} is in \mathcal{SF}_c , the arguments of all the integrals in the right-hand side above are polynomials. Using the degrees of freedom of \mathbf{v} it is possible to reconstruct $\operatorname{div} \mathbf{v}$ inside c and $\mathbf{v} \cdot \mathbf{n}_f$ on each $f \in \partial c$, see [30], and all these integrals are computable. Combining the last formulas, we obtain the algebraic form of the consistency condition:

$$[(\mathbb{K}_c \nabla q)^I, \mathbf{v}_c^I]_{\mathcal{F}_{h,c}} = ((\mathbb{K}_c \nabla q)^I)^T \mathbf{M}_{\mathcal{F},c} \mathbf{v}_c^I = (\mathbf{r}_c(q))^T \mathbf{v}_c^I.$$

To find a symmetric positive definite matrix $\mathbf{M}_{\mathcal{F},c}$, we need the analog of Lemma 3.1, which obviously holds since the function $\mathbb{K}_c \nabla \tilde{q}$ is in the space \mathcal{SF}_c for any polynomial $\tilde{q} \in \mathcal{P}^{r+2}(c)$.

In the third step, we formulate the duality formula for the derived gradient operator and use it in the global mimetic formulation. The following error estimates have been shown in [30]:

$$\| \| p^I - p_h \| \|_{\mathcal{C}_h} + \| \| \mathbf{u}^I - \mathbf{u}_h \| \|_{\mathcal{F}_h} \leq C h^{r+2}.$$

Remark 4.1 *In the case when the diffusion tensor \mathbb{K} is no longer constant, the consistency condition has to be modified. Let Π_c^r denote the local L^2 projector on the space of polynomial functions of order r . Then, the modified consistency condition reads:*

$$[(\Pi_c^{r+1}(\mathbb{K} \nabla q))^I, \mathbf{v}_c^I]_{\mathcal{F}_{h,c}} = \int_c \nabla q \cdot \mathbf{v} \, dx \quad \forall q \in \mathcal{P}^{r+2}(c), \forall \mathbf{v} \in \mathcal{SF}_c.$$

After that, the inner product matrix $\mathbf{M}_{\mathcal{F},c}$ is derived following the same steps.

4.2 Nonlinear parabolic problems

The consistency term in the formula for matrix $\mathbf{M}_{\mathcal{F},c}$ (see (3.9)) contains the inverse of the diffusion tensor. Therefore, numerical difficulties may arise in solving nonlinear parabolic problems of type

$$\frac{\partial p}{\partial t} - \operatorname{div}(k(p) \nabla p) = b,$$

where function $k(p)$ cannot be uniformly bounded from below. For instance, on a uniform one dimensional mesh, the numerical flux at mesh point x_i is proportional to the difference of the neighboring pressures and the transmissibility coefficient T_i :

$$u_i = -T_i \frac{p_{i+1/2} - p_{i-1/2}}{h}, \quad T_i = \frac{2 k_{i-1/2} k_{i+1/2}}{k_{i-1/2} + k_{i+1/2}}.$$

If $k_{i-1/2} \ll k_{i+1/2}$, the numerical flux goes to zero as $k_{i-1/2} \rightarrow 0$ and may lead to a nonphysical solution as shown by the numerical experiment considered in Section 4.2.2 (see also [40]). To obtain an accurate solution, we have to replace the harmonic average with the arithmetic average in the definition of the transmissibility coefficient. A possible strategy in the mixed finite element framework (see, e.g. [4]) consists in using two velocity variables, $\mathbf{v} = -\nabla p$ and $\mathbf{u} = k(p)\mathbf{v}$. However, the corresponding weak formulation cannot have face-based equations of type $v_c^f = k_f u_c^f$ which are natural from a physical viewpoint. Here k_f is the face-based diffusion coefficient. Such face-based equations lead to an algebraic problem that can be symmetrized only on special meshes. We describe a new mimetic scheme that allows us to use different values k_f on different mesh faces. The mimetic framework always guarantees the symmetry of the resulting algebraic problem.

4.2.1 A new pair of primary and derived mimetic operators

Let us consider a more general form of the diffusion coefficient, $\mathbb{K}k(p)$, where \mathbb{K} is a discontinuous tensor independent of p and $k(p)$ is a discontinuous scalar function of p . The underlying mixed formulation is

$$\begin{aligned} \mathbf{u} &= -(\mathbb{K} \nabla) p, \\ \frac{\partial p}{\partial t} + (\operatorname{div} k) \mathbf{u} &= b. \end{aligned} \tag{4.1}$$

The combined operators $\operatorname{div} k$ and $\mathbb{K} \nabla$ are dual to each other with respect to the weighted L^2 inner products by using $k\mathbb{K}^{-1}$ as weight:

$$\int_{\Omega} (\operatorname{div} k \mathbf{u}) q \, dx = - \int_{\Omega} k \mathbb{K}^{-1} \mathbf{u} \cdot (\mathbb{K} \nabla) q \, dx \quad \forall \mathbf{u} \in H_{\operatorname{div}}(\Omega), \quad \forall q \in H_0^1(\Omega). \tag{4.2}$$

Consider again the three-step construction of the mimetic framework. In the *first* step we need to specify the degrees of freedom. For the pressure variable, we consider the same discrete space \mathcal{C}_h of grid functions that consist of one value per cell and the same discrete space Λ_h of grid functions that consist of one value per face. The discrete space \mathcal{F}_h has the same dimension as in the linear case, but the discrete fluxes in \mathcal{F}_h obey a different continuity condition:

$$k_f^{c_1} u_f^{c_1} = k_f^{c_2} u_f^{c_2} \tag{4.3}$$

on each interior face f shared by cells c_1 and c_2 . Here, $k_f^{c_1}$ and $k_f^{c_2}$ are accurate one-side approximations of the diffusion coefficient k . For example, in regions where function k is continuous, we can take $k_f^{c_1} = k_f^{c_2} = k_f$ as a weighted average of the cell-centered values $k(p_{c_1})$ and $k(p_{c_2})$ calculated using the most recent approximation to solution p in the cells c_1 and c_2 , respectively. The weights are the distances between the cell centers and face f .

The primary mimetic operator approximates the combined operator $\operatorname{div} k$. It is defined locally on each mesh cell using a straightforward discretization of the divergence theorem (compare with formula (3.7)):

$$(\mathcal{DIV}^k \mathbf{u}_h)|_c \equiv \mathcal{DIV}_c^k \mathbf{u}_c = \frac{1}{|c|} \sum_{f \in \partial c} \sigma_{c,f} |f| k_f^c u_f^c. \quad (4.4)$$

Since \mathbf{u}_h is an algebraic vector, it is convenient to think about the discrete divergence operator $\mathcal{DIV}^k: \mathcal{F}_h \rightarrow \mathcal{P}_h$ as a matrix acting between two spaces. This matrix has full rank when $k_f^c > 0$.

Let us introduce a cell-based diagonal matrix \mathcal{K}_c formed by coefficients k_f^c , $f \in \partial c$. Then, the primary mimetic operators in (3.7) and (4.4) can be connected as follows:

$$\mathcal{DIV}_c^k \mathbf{u}_c = (\mathcal{DIV}_c \mathcal{K}_c) \mathbf{u}_c.$$

The *second* step in the mimetic discretization framework is to define the inner products in spaces \mathcal{C}_h and \mathcal{F}_h that are accurate approximations of the integrals in (4.2). Such inner products can be defined again cell-by-cell. Moreover, the inner product in space \mathcal{C}_h can be defined as in Section 3.2 by the relation $[p_c, q_c]_{\mathcal{C}_{h,c}} = |c| p_c q_c$.

The weight in the other L^2 inner product is given by $k \mathbb{K}^{-1}$. By our assumption, \mathbb{K} is a piecewise constant tensor on mesh Ω_h . Instead, the scalar coefficient k can be a quite general non-negative function. An acceptable first-order error is committed when we replace k by the piecewise constant function with value $k_c = k(p_c)$ in cell c .

The consistency condition is expressed through the exactness property:

$$[\mathbf{u}_c^I, \mathbf{v}_c^I]_{\mathcal{F}_{h,c}} = \int_c k(p_c) \mathbb{K}_c^{-1} \mathbf{u} \cdot \mathbf{v} \, dx \quad \forall \mathbf{u} \in (\mathcal{P}^0(c))^d, \forall \mathbf{v} \in \mathcal{SF}_c.$$

Since $k_c \mathbb{K}_c^{-1}$ is a constant tensor in cell c , the derivation of the inner product matrix (still denoted by $\mathbf{M}_{\mathcal{F},c}$) proceeds as in Section 3.2.

The *third* step in the construction of the mimetic framework is to obtain the formula for the derived operator, which, in this case, is an approximation of the combined operator $\mathbb{K} \nabla$. The continuum Green formula for cell c is given by

$$\int_c (\operatorname{div} k \mathbf{u}) q \, dx - \int_{\partial c} (k \mathbf{u} \cdot \mathbf{n}) q \, dx = - \int_c k \mathbb{K}^{-1} (\mathbb{K} \nabla q) \cdot \mathbf{u} \, dx. \quad (4.5)$$

Now, the derived operator $\widetilde{\mathcal{GRAD}}_c: \mathcal{C}_{h,c} \times \Lambda_{h,c} \rightarrow \mathcal{F}_{h,c}$ satisfies the discrete integration by parts formula

$$[\mathcal{DIV}_c^k \mathbf{u}_c, q_c]_{\mathcal{C}_{h,c}} - \sum_{f \in \partial c} \sigma_{c,f} |f| k_f^c u_f^c \lambda_f = - \left[\mathbf{u}_c, \widetilde{\mathcal{GRAD}}_c \begin{pmatrix} q_c \\ \boldsymbol{\lambda}_c \end{pmatrix} \right]_{\mathcal{F}_{h,c}}$$

for all $\mathbf{u}_c \in \mathcal{F}_{h,c}$, $q_c \in \mathcal{C}_{h,c}$, and $\boldsymbol{\lambda}_c \in \Lambda_{h,c}$. This local mimetic formulation gives the following formula for the physical fluxes:

$$\mathcal{K}_c \begin{pmatrix} u_{f_1}^c \\ \vdots \\ u_{f_{n_c}}^c \end{pmatrix} = -\mathcal{K}_c \widetilde{\mathcal{GRAD}}_c \begin{pmatrix} p_c \\ \boldsymbol{\lambda}_c \end{pmatrix} = \mathcal{K}_c \mathbf{M}_{\mathcal{F},c}^{-1} \mathcal{K}_c \begin{pmatrix} \sigma_{c,f_1} |f_1|(p_c - \lambda_{f_1}) \\ \vdots \\ \sigma_{c,f_{n_c}} |f_{n_c}|(p_c - \lambda_{f_{n_c}}) \end{pmatrix}. \quad (4.6)$$

Note that this formula uses the symmetric matrix $\mathcal{K}_c \mathbf{M}_{\mathcal{F},c}^{-1} \mathcal{K}_c$. Our numerical experiments show that the resulting scheme is second-order accurate.

4.2.2 Marshak heat equation

Let us consider the modified Marshak heat equation [44, 40] in the rectangular domain $(0, 3) \times (0, 1)$ with zero source term, $\mathbb{K} = 1$, and $k(p) = p^3$. The initial value is $p(\mathbf{x}, 0) = 10^{-3}$. We set the time-dependent Dirichlet boundary condition $p = p^0(0, t) = 0.78 t^{1/3}$ on the left side of Ω , the constant boundary condition $p = 10^{-3}$ on the right side, and the homogeneous Neumann boundary conditions on the remaining sides.

We solve the parabolic equation on the randomly perturbed quadrilateral mesh that have three times more cells in the x-direction than in the y-direction. We use the backward Euler time integration scheme and the weighted arithmetic average definition of the face-based diffusion coefficients k_f described above. To reduce the impact of the time integration error, we use small time steps. Comparison of pictures in Fig. 4 show that the new scheme fixes the deficiencies of the old MFD scheme and leads to the correct speed of propagation of the non-linear wave.

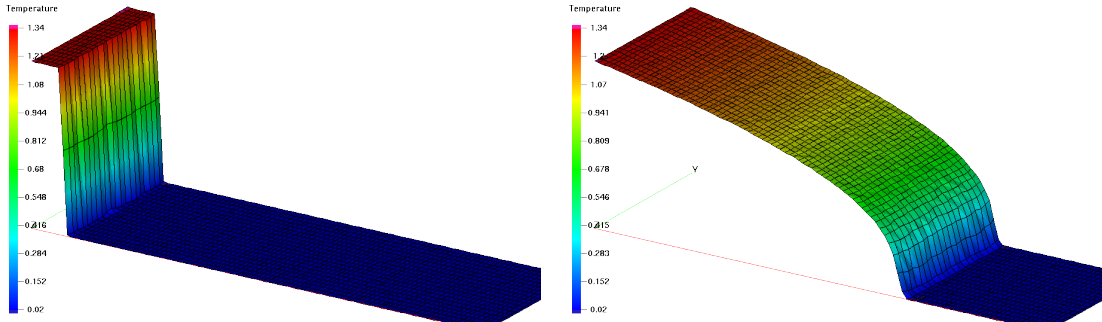


Figure 4: Solution snapshots at time $t = 5.0$ for the standard (left) and new (right) MFD schemes. The solution in the right panel shows the correct and accurate position of the wave front at the chosen time.

5 Conclusions

We described a few design principles used in the derivation of mimetic schemes for the numerical solution of PDEs. We established the bridges with a few FV and FE methods by

showing that three popular discretization frameworks (MFD, FV and FE) use the equivalent design principles which leads to algebraically equivalent schemes. We illustrated the flexibility of the mimetic discretization framework to tackle challenging numerical issues in computer modeling of engineering problems with two examples: derivation of higher-order schemes and convergent schemes for nonlinear problems with small diffusion coefficients.

Acknowledgments

This work was carried out under the auspices of the National Nuclear Security Administration of the U.S. Department of Energy at Los Alamos National Laboratory under Contract No. DE-AC52-06NA25396. The authors acknowledge the support of the US Department of Energy Office of Science Advanced Scientific Computing Research (ASCR) Program in Applied Mathematics Research.

The meshes for the Marshak problem were created and managed using the mesh generation toolset MSTK (software.lanl.gov/MeshTools/trac) developed by Dr. Rao Garimella at Los Alamos National Laboratory.

References

- [1] P. Antonietti, L. Beirão da Veiga, and M. Verani. A mimetic discretization of elliptic obstacle problems. *Math. Comp.*, 82:1379–1400, 2013.
- [2] P. F. Antonietti, L. Beirão da Veiga, N. Bigoni, and M. Verani. Mimetic finite differences for nonlinear and control problems. *Mathematical Models and Methods in Applied Sciences*, 24(08):1457–1493, 2014.
- [3] P. F. Antonietti, N. Bigoni, and M. Verani. Mimetic discretizations of elliptic control problems. *J. Sci. Comput.*, 56(1):14–27, 2013.
- [4] T. Arbogast, M. Wheeler, and I. Yotov. Mixed finite elements for elliptic problems with tensor coefficients as cell-centered finite difference. *SIAM J. Numer. Anal.*, 34(2):828–852, 1997.
- [5] L. Beirão da Veiga. A mimetic finite difference method for linear elasticity. *ESAIM: Mathematical Modelling and Numerical Analysis*, 44(2):231–250, 2010.
- [6] L. Beirão da Veiga, J. Droniou, and G. Manzini. A unified approach to handle convection term in finite volumes and mimetic discretization methods for elliptic problems. *IMA Journal on Numerical Analysis*, 31(4):1357–1401, 2011.
- [7] L. Beirão da Veiga, V. Gyrya, K. Lipnikov, and G. Manzini. Mimetic finite difference method for the Stokes problem on polygonal meshes. *J. Comp. Phys.*, 228(19):7215–7232, 2009.
- [8] L. Beirão da Veiga, K. Lipnikov, and G. Manzini. Error analysis for a mimetic discretization of the steady Stokes problem on polyhedral meshes. *SIAM J. Numer. Anal.*, 48(4):1419–1443, 2010.

- [9] L. Beirão da Veiga, K. Lipnikov, and G. Manzini. *The Mimetic Finite Difference Method*, volume 11 of *Modeling, Simulations and Applications*. Springer-Verlag, New York, I edition, 2014.
- [10] L. Beirão da Veiga and D. Mora. A mimetic discretization of the Reissner–Mindlin plate bending problem. *Numerische Mathematik*, 117(3):425–462, 2011.
- [11] P. Bochev and J. M. Hyman. Principle of mimetic discretizations of differential operators. In D. Arnold, P. Bochev, R. Lehoucq, R. Nicolaides, and M. Shashkov, editors, *Compatible discretizations. Proceedings of IMA hot topics workshop on compatible discretizations*, IMA Volume 142. Springer-Verlag, 2006.
- [12] F. Brezzi, A. Buffa, and G. Manzini. Mimetic scalar products of discrete differential forms. *J. Comp. Phys.*, 257, Part B(0):1228–1259, 2014.
- [13] F. Brezzi, R. Falk, and L. Marini. Basic principle of mixed virtual element methods. *ESAIM: Mathematical Modelling and Numerical Analysis*, 48(1):1227–1240, 2014.
- [14] F. Brezzi, K. Lipnikov, and M. Shashkov. Convergence of the mimetic finite difference method for diffusion problems on polyhedral meshes. *SIAM J. Numer. Anal.*, 43(5):1872–1896, 2005.
- [15] A. Cangiani, F. Gardini, and G. Manzini. Convergence of the mimetic finite difference method for eigenvalue problems in mixed form. *Computer Methods in Applied Mechanics and Engineering*, 200(9-12):1150–1160, 2011.
- [16] A. Cangiani and G. Manzini. Flux reconstruction and pressure post-processing in mimetic finite difference methods. *Computer Methods in Applied Mechanics and Engineering*, 197(9-12):933–945, 2008.
- [17] A. Cangiani, G. Manzini, and A. Russo. Convergence analysis of the mimetic finite difference method for elliptic problems. *SIAM J. Numer. Anal.*, 47(4):2612–2637, 2009.
- [18] J. Castor. *Radiation Hydrodynamics*. Cambridge University Press, 2004.
- [19] B. Cockburn, J. Gopalakrishnan, and R. Lazarov. Unified hybridization of discontinuous Galerkin, mixed, and continuous Galerkin methods for second order elliptic problems. *SIAM J. Numer. Anal.*, 47(2):1319–1365, 2009.
- [20] Y. Coudière and G. Manzini. The Discrete Duality Finite Volume method for convection-diffusion problems. *SIAM J. Numer. Anal.*, 47(6):4163–4192, 2010.
- [21] D. A. Di Pietro and A. Ern. *Mathematical Aspects of Discontinuous Galerkin Methods*. Mathématiques et Applications. Springer, 2011.
- [22] D. A. Di Pietro and A. Ern. Hybrid high-order methods for variable diffusion problems on general meshes. *Comptes Rendus Mathématique*, 353:31–34, July 2014.

- [23] K. Domelevo and P. Omnes. A finite volume method for the Laplace equation on almost arbitrary two-dimensional grids. *ESAIM: Mathematical Modelling and Numerical Analysis*, 39(6):1203–1249, 2005.
- [24] J. Droniou. Finite volume schemes for diffusion equations: Introduction to and review of modern methods. *Mathematical Models and Methods in Applied Sciences*, 24(08):1575–1619, 2014.
- [25] J. Droniou and R. Eymard. A mixed finite volume scheme for anisotropic diffusion problems on any grid. *Numerische Mathematik*, 1(105):35–71, 2006.
- [26] J. Droniou, R. Eymard, T. Gallouët, and R. Herbin. A unified approach to mimetic finite difference, hybrid finite volume and mixed finite volume methods. *Mathematical Models and Methods in Applied Sciences*, 20(2):265–295, 2010.
- [27] G. M. Dusinberre. Heat transfer calculations by numerical methods. *Journal of the American Society for Naval Engineers*, 67(4):991–1002, 1955.
- [28] G. M. Dusinberre. *Heat-transfer calculation by finite differences*. International Textbook Company, Scranton, Pennsylvania, 1961.
- [29] R. Eymard, T. Gallouët, and R. Herbin. Discretization of heterogeneous and anisotropic diffusion problems on general nonconforming meshes. SUSI: a scheme using stabilization and hybrid interfaces. *IMA Journal of Numerical Analysis*, 30(4):1009–1043, 2010.
- [30] V. Gyrya, K. Lipnikov, and G. Manzini. The arbitrary order mixed mimetic finite difference method for the diffusion equation. Technical Report LA-UR-15-00000, Los Alamos National Laboratory, 2015. Submitted to *Mathematical Modelling and Numerical Analysis*.
- [31] J. Hyman and M. Shashkov. The approximation of boundary conditions for mimetic finite difference methods. *Comput. Math. Appl.*, 36:79–99, 1998.
- [32] J. Hyman and M. Shashkov. Mimetic discretizations for Maxwell’s equations and the equations of magnetic diffusion. *Progress in Electromagnetic Research*, 32:89–121, 2001.
- [33] J. Hyman, M. Shashkov, and S. Steinberg. The numerical solution of diffusion problems in strongly heterogeneous non-isotropic materials. *J. Comp. Phys.*, 132(1):130–148, 1997.
- [34] K. Lipnikov, G. Manzini, F. Brezzi, and A. Buffa. The mimetic finite difference method for 3D magnetostatics fields problems. *J. Comp. Phys.*, 230(2):305–328, 2011.
- [35] K. Lipnikov, G. Manzini, and M. Shashkov. Mimetic finite difference method. *J. Comp. Phys.*, 257, Part B(0):1163–1227, 2014.

- [36] K. Lipnikov, J. Moulton, and D. Svyatskiy. A Multilevel Multiscale Mimetic (M^3) method for two-phase flows in porous media. *J. Comp. Phys.*, 227:6727–6753, 2008.
- [37] K. Lipnikov, M. Shashkov, and I. Yotov. Local flux mimetic finite difference methods. *Numerische Mathematik*, 112(1):115–152, 2009.
- [38] G. Manzini, A. Russo, and N. Sukumar. New perspectives on polygonal and polyhedral finite element methods. *Mathematical Models and Methods in Applied Sciences*, 24(8):1665–1699, 2014.
- [39] L. Margolin, M. Shashkov, and P. Smolarkiewicz. A discrete operator calculus for finite difference approximations. *Computer Methods in Applied Mechanics and Engineering*, 187(3-4):365–383, 2000.
- [40] V. I. Maslyankin. Convergence of the iterative process for the quasilinear heat transfer equation. *USSR Comput. Math. Math. Phys.*, 17(1):201–210, 1977.
- [41] A. Palha, P. P. Rebelo, R. Hiemstra, J. Kreeft, and M. Gerritsma. Physics-compatible discretization techniques on single and dual grids, with application to the Poisson equation of volume forms. *J. Comp. Phys.*, 257, Part B(0):1394–1422, 2014.
- [42] P. Raviart and J. Thomas. A mixed finite element method for second order elliptic problems. In I. Galligani and E. Magenes, editors, *Math. Aspects of Finite Element Method, Lecture Notes in Math. 606*. Springer-Verlag, N.Y., 1977.
- [43] L. Richards. Capillary conduction of liquids through porous mediums. *Physics 1*, 5:318–333, 1931.
- [44] A. Samarskii and I. Sobol'. Examples of the numerical calculation of temperature waves. *USSR Comput. Math. Math. Phys.*, 3(4):945–970, 1963.
- [45] N. Sukumar and E. A. Malsch. Recent advances in the construction of polygonal finite element interpolants. *Archives of Computational Methods in Engineering*, 13(1):129–163, 2006.
- [46] N. Sukumar and A. Tabarraei. Conforming polygonal finite elements. *Int. J. Numer. Meth. Engrg.*, 61(12):2045–2066, 2004.
- [47] A. Tabarraei and N. Sukumar. Application of polygonal finite elements in linear elasticity. *Int. J. Comp. Mech.*, 3(4):503–520, 2006.
- [48] E. Wachspress. *A Rational Finite Element Basis*. Academic Press, 1975.
- [49] J. Wang and X. Ye. A weak Galerkin mixed finite element method for second order elliptic problems. *Math. Comp.*, 83:2101–2126, 2014.